Research Square

Preprints are preliminary reports that have not undergone peer review.
They should not be considered conclusive, used to inform clinical practice,
or referenced by the media as validated information.

Spatial Estimation of Near-surface Density From Gravity–topography Relationships Using Nettleton Analysis and a Moving-window Parasnis Approach

Nelson Ribeiro-Filho

nelson.filho@ifpa.edu.br

IFPA: Instituto Federal de Educacao Ciencia e Tecnologia do Para https://orcid.org/0000-0002-4029-5013

Mauricio Amorim

IFPA: Instituto Federal de Educacao Ciencia e Tecnologia do Para

Luiz Antônio Melo Viegas

IFPA: Instituto Federal de Educacao Ciencia e Tecnologia do Para

Valdeides Marques Lima

IFPA: Instituto Federal de Educacao Ciencia e Tecnologia do Para

Research Article

Keywords: near-surface density, gravity–topography relationship, Parasnis method, Nettleton method, moving-window analysis

Posted Date: September 29th, 2026

DOI: https://doi.org/10.21203/rs.3.rs-10483618/v1

License: This work is licensed under a Creative Commons Attribution 4.0 International License.
Read Full License

SPATIAL ESTIMATION OF NEAR-SURFACE DENSITY FROM GRAVITY–TOPOGRAPHY RELATIONSHIPS USING NETTLETON ANALYSIS AND A MOVING-WINDOW PARASNIS APPROACH

Nelson Ribeiro-Filho[1*]

Instituto Federal de Educação, Ciência e Tecnologia do Pará – Campus Altamira

nelson.filho@ifpa.edu.br; nelsondelimar@gmail.com

https://orcid.org/0000-0002-4029-5013

Maurício da Silva Amorim[1]

Instituto Federal de Educação, Ciência e Tecnologia do Pará – Campus Altamira

mauricio.amorim@ifpa.edu.br

https://orcid.org/0009-0006-0857-1619

Luiz Antônio Melo Viegas[1]

Instituto Federal de Educação, Ciência e Tecnologia do Pará – Campus Altamira

luiz.viegas@ifpa.edu.br

https://orcid.org/0009-0005-6903-8167

Valdeides Marques Lima[2]

Instituto Federal de Educação, Ciência e Tecnologia do Pará – Campus Castanhal

valdeides.lima@ifpa.edu.br

https://orcid.org/0000-0002-0401-4982

* Corresponding author

ABSTRACT

Near-surface density is essential for gravity correction and the interpretation of shallow mass variations, but classical gravity–topography methods generally provide only a single representative value for an entire profile or survey area. This study develops a spatial workflow that extends the Parasnis formulation to local moving-window regression over gridded datasets, while retaining the Nettleton and global Parasnis methods as reference estimators. The approach was first assessed using a controlled two-dimensional synthetic model with lateral variations in topography, density, and gravity response. Although local pointwise deviations remained, the moving-window solution preserved the dominant spatial organization of the reference density field and recovered its principal density-related compartments. The method was subsequently applied to topographic and Bouguer anomaly data from the Altamira region, northern Brazil. After applying physically plausible bounds, the local Parasnis analysis produced a spatially coherent empirical density field, and the corresponding local-correlation map provided an auxiliary measure of the stability of the gravity–topography relationship. The results show that local gravity–topography regression can extend classical representative-density estimation into a spatially distributed framework for identifying relative mass-related contrasts. The recovered values should be interpreted as empirical density indicators rather than direct measurements. The workflow is computationally simple, transferable to other gridded gravity datasets, and potentially useful for applied, environmental, and near-surface geophysical investigations.

Key-words: near-surface density; gravity–topography relationship; Parasnis method; Nettleton method; moving-window analysis.

1 INTRODUCTION

Density is a fundamental physical property in geophysics because it controls mass distribution and directly influences the gravitational response of near-surface and subsurface materials. Spatial density variations are commonly associated with changes in lithology, degree of weathering, porosity, compaction, moisture content, and structural organization, making density essential for gravity correction, forward modeling, inversion, and geological interpretation (Blakely 1996; Hinze et al. 2013; Roy 2007; Telford et al. 1990). In shallow investigations, density is also closely related to the physical condition of soils and unconsolidated materials, as it reflects variations in pore-space arrangement, mechanical resistance, water-storage capacity, and horizon development. For this reason, density has long been recognized as a relevant parameter not only in geophysical studies but also in environmental, pedological, hydrogeological, and land-use investigations (Coutinho 2019; Cunha et al. 2018; Freitas et al. 2018; Gouveia and Nobre 2016; Pádua et al. 2015; Pimenta 2018; Uchôa et al. 2011).

Over the last decades, the growing demand for spatially distributed information on shallow materials has stimulated the integration of geophysics with soil science, environmental monitoring, and agricultural studies. This development has contributed to the consolidation of agrogeophysics as an interdisciplinary field that uses geophysical observations to investigate soil properties, landscape dynamics, hydrological behavior, crop-related processes, and subsurface heterogeneity in managed environments (Allred et al. 2008, 2010, 2016; Garré et al. 2017, 2021; Romero-Ruiz et al. 2025). In this broader context, geophysical methods have increasingly been employed as non-destructive tools for characterizing the shallow subsurface, complementing direct sampling, and supporting spatial interpretation where conventional point measurements are sparse or logistically limited (Groves et al. 2011; Luna and Jadi 2000; Romero-Ruiz et al. 2018).

A wide range of studies has shown that geophysical data can provide relevant information on soil structure, compaction, texture, water dynamics, shallow stratigraphy, and other properties of environmental and agricultural interest. Electrical and electromagnetic methods have been widely used to investigate apparent electrical conductivity, salinity, soil–water interactions, and spatial variability associated with agronomic management zones (Brown et al. 2021; Corwin 2008; Farifteh et al. 2006; von Hebel et al. 2021). Time-lapse geophysical approaches have also been successfully applied to assess soil-moisture dynamics and the effects of agricultural practices on shallow water redistribution (Blanchy et al. 2020). Integrated geophysical frameworks have further contributed to the investigation of soil pipes, compaction, root-water uptake, and hydrodynamic behavior in structured soils (Cimpoiașu et al. 2021; Kuhl et al. 2021; Samad et al. 2022). Seismic and other near-surface geophysical methods have likewise been used to assess soil-compaction levels, bedrock depth, and shallow stratigraphic architecture, reinforcing the practical

importance of indirect techniques for characterizing heterogeneous terrains (Barboza-Miranda et al. 2025; Carrera et al. 2024; Julyani et al. 2025; Siregar et al. 2026).

The interpretation of soil-related geophysical data has advanced considerably through the integration of geophysical measurements with geostatistics, remote sensing, unmanned aerial vehicle products, machine learning, agrogeological information, and direct soil observations. Geophysical and geostatistical techniques have been combined to map the spatial variation of clay content (De Benedetto et al. 2012), whereas agrogeophysical and agrogeological approaches have been applied to estimate soil clay content in heterogeneous environments (Kritikakis et al. 2022). Remote sensing, solute modeling, and geophysical observations have also been integrated to assess salt-affected soils (Farifteh et al. 2006), while geophysical techniques combined with unmanned aerial vehicle mapping have been used to detect and monitor soil pipes and collapse features in agricultural landscapes (Hosseinalizadeh et al. 2025). More recently, machine learning, geophysical data, and field measurements have been integrated to predict wetland soil properties (Driba et al. 2024), and agrogeophysical approaches have been applied to estimate A-horizon thickness in long-term cropping systems (Ramos et al. 2026). These developments illustrate the growing role of geophysics in providing spatially continuous information for interpreting near-surface variability in environmental and agricultural investigations (Krüger et al. 2013; O'Leary et al. 2026).

The expansion of geophysical applications has reinforced the understanding that indirect geophysical observables can provide valuable information even when the target property is not measured directly. Reviews and perspective studies have emphasized that one of the central challenges in agrogeophysics is transforming indirect measurements into physically meaningful spatial estimates of soil and near-surface attributes (Garré et al. 2017, 2021; Romero-Ruiz et al. 2018, 2025). This challenge involves not only water-related variables and conductivity-based indicators but also structural and mechanical properties, including compaction, pore-system organization, mineralogical contrasts, and density-related variability (Carrera et al. 2024; Menshov et al. 2012; Siregar et al. 2026). In this context, density is particularly relevant because it is physically linked to the gravitational field and, at the same time, associated with porosity trends, material compactness, and the internal organization of shallow layers.

Among the available geophysical observables, gravity data are particularly suitable for empirical density analysis because they respond directly to mass distribution. This physical relationship makes gravimetry relevant to near-surface investigations in which representative density values are required for Bouguer correction, anomaly interpretation, and preliminary characterization of shallow materials. The importance of laterally variable density models has also been emphasized in recent gravimetric studies, which show that spatial density variations can significantly affect the accuracy of gravity corrections and the interpretation of complex geological settings (Nergizci et al. 2024; Niu et al. 2025). Although gravimetry is more commonly associated with crustal- and basin-scale investigations, its direct sensitivity to density

makes it a useful tool for empirical density estimation when combined with topographic information in shallow and regional applications.

Classical gravity-based strategies for empirical density estimation are traditionally represented by the Nettleton and Parasnis methods. In the Nettleton method, density is estimated by identifying the value that minimizes the relationship between Bouguer anomaly and elevation along a profile (Nettleton 1939). The Parasnis method expresses the same physical principle through a regression-based relationship between gravity and topography, from which density can be estimated analytically from the slope of the fitted line (Orihuela 1997; Parasnis 1997). Both methods are conceptually simple, computationally inexpensive, and physically interpretable, which explains their continued relevance in empirical density studies. However, most traditional applications remain focused on profile-based analyses and on determining a single representative density for a given area (Nettleton 1939; Orihuela 1997; Parasnis 1997). This is an important limitation because modern near-surface datasets are commonly organized as regular grids, whereas shallow materials rarely behave as laterally homogeneous media. Soil and regolith properties may vary substantially over short distances because of differences in texture, weathering, moisture conditions, compaction, stratigraphic organization, and land-use history, as documented in several near-surface and soil-characterization studies (Carrera et al. 2024; De Benedetto et al. 2012; Driba et al. 2024; Julyani et al. 2025; Kritikakis et al. 2022; Ramos et al. 2026). Under such conditions, a single density value may be insufficient to represent local variability, whereas moving-window estimates may provide a more informative representation of the spatial behavior of the shallow subsurface.

This limitation is particularly relevant in near-surface density studies because density may serve as a first-order indicator of material organization and may also be interpreted, with appropriate caution, in relation to compaction and porosity trends. Although the present study does not aim to produce porosity maps as a primary result, the physical relationship between density and pore-space distribution reinforces the broader value of obtaining spatially coherent density patterns from gravity–topography relationships. This interpretative perspective is consistent with recent studies in agrogeophysics and near-surface geophysics, in which geophysical information has been used to support the analysis of soil structure, compaction, root-zone behavior, moisture dynamics, shallow stratigraphy, and other properties related to the physical organization of the subsurface (Blanchy et al. 2020; Brown et al. 2021; Cimpoiașu et al. 2021; Garré et al. 2021; Kuhl et al. 2021; O'Leary et al. 2026; Romero-Ruiz et al. 2018, 2025; Samad et al. 2022; Siregar et al. 2026).

In this context, the present study investigates the empirical estimation of near-surface density from gravity–topography relationships using the classical Nettleton and Parasnis methods, with particular emphasis on extending the Parasnis formulation to local moving-window analysis over gridded datasets. The proposed workflow is first evaluated through a controlled two-dimensional synthetic experiment in

147 which the reference density field is known, allowing the spatial behavior of the local estimates to be assessed
148 directly. A representative profile extracted from the synthetic model is then used to compare the global
149 Nettleton and Parasnis estimates with the spatially variable local Parasnis solution. Finally, the methodology
150 is applied to real topographic and gravimetric data from northern Brazil to examine its practical performance
151 under natural conditions. By transforming a classical representative-density estimator into a spatially
152 distributed framework, the study seeks to provide a computationally simple and physically interpretable
153 approach for identifying relative density contrasts in heterogeneous shallow environments. The resulting
154 values are interpreted as empirical density indicators rather than direct measurements, and their potential
155 applications include applied, environmental, and near-surface geophysical investigations.
156
157 **2 MATERIALS AND METHODS**
158 **2.1 Physical basis of the gravity–topography relationship**
159 The Nettleton and Parasnis methods are based on the gravitational effect of topographic masses. In
160 gravity surveys, the observed field contains contributions from both shallow and deep sources, and part of
161 the signal measured in areas of significant relief is associated with the mass excesses and deficiencies
162 produced by topography. Because the magnitude of this contribution depends on the density of the near-
163 surface materials, the relationship between gravity and topography can be used to estimate an empirical
164 representative density for the analyzed domain (Blakely 1996; Hinze et al. 2013; Roy 2007; Telford et al.
165 1990).
166 Let g_{obs} denote the observed gravity at an elevation h. A corrected gravity anomaly may be expressed
167 as
168 $$\Delta g = g_{Obs} - g_{th} + \delta g_{FA} - \delta g_{BG} \quad (1)$$
169 where g_{th} is the theoretical gravity, δg_{FA} is the free-air correction, and δg_{BG} is the Bouguer
170 correction. Under the infinite-slab approximation, the Bouguer correction is given by
171 $$\delta g_{BG} = 2\pi G\rho h \quad (2)$$
172 where G is the gravitational constant and ρ is the density assigned to the topographic masses.
173 Therefore,
174 $$\Delta g = g_{Obs} - g_{th} + \delta g_{FA} - 2\pi G\rho h \quad (3)$$
175 Equation (3) shows that the corrected gravity anomaly depends explicitly on the adopted density. If the
176 tested density is too low, the topographic effect is undercorrected and the residual anomaly retains a
177 systematic relationship with relief. Conversely, if the density is too high, the correction is excessive and the
178 anomaly may develop an opposite trend with elevation. The most appropriate empirical density is therefore
179 the value that minimizes the residual dependence between the corrected gravity anomaly and topography.
180 This principle provides the common physical basis of the Nettleton and Parasnis methods.

2.2 Nettleton method

The Nettleton method is a classical procedure for estimating a representative near-surface density from gravity observations acquired over variable relief (Nettleton 1939; Hinze et al. 2013). Its underlying principle is that, when the appropriate density is used in the Bouguer correction, the corrected gravity anomaly should exhibit minimum systematic dependence on topography. The method therefore evaluates a set of candidate densities and identifies the value that most effectively removes the correlation between corrected anomaly and elevation.

For a tested density ρ_j, the corrected anomaly at the i-th observation may be written as

$$\Delta g_i(\rho_j) = g_{obs,i} - g_{th,i} + \delta g_{FA,i} - 2\pi G \rho_j h_i \tag{4}$$

where h_i is the elevation of the observation point. A set of candidate densities ρ_1, ρ_2, ..., ρ_m is evaluated, and the relationship between elevation and corrected anomaly is quantified for each candidate using the Pearson correlation coefficient:

$$r(p_j) = \frac{\sum_{i=1}^{N}\left(\Delta g_i(\rho_j) - \overline{\Delta g_i(\rho_j)}\right)\cdot\left(h_i - \overline{h}\right)}{\sqrt{\sum_{i=1}^{N}\left(\Delta g_i(\rho_j) - \overline{\Delta g_i(\rho_j)}\right)^2}\cdot\sqrt{\sum_{i=1}^{N}\left(h_i - \overline{h}\right)^2}} \tag{5}$$

where $\overline{h}$ is the mean elevation and $\overline{\Delta g_i(\rho_j)}$ is the mean corrected anomaly obtained for the tested density ρ_j.

The Nettleton density estimate is therefore defined as

$$\rho^* = \arg\min_{\rho_j}\left|r(p_j)\right| \tag{6}$$

This formulation preserves the original physical basis of the Nettleton method while replacing subjective visual comparison with an explicit and reproducible statistical criterion. In practice, the method is particularly suitable for profile-based analysis and for estimating a single representative density over a finite set of observations.

2.3 Parasnis method

The Parasnis method expresses the same physical principle in analytical form by estimating density directly from the linear relationship between gravity anomaly and elevation (Orihuela 1997; Parasnis 1997). For a given set of observations, this relationship may be represented as

$$\Delta g_i = \beta_0 + \beta_1 h_i + \epsilon_i \tag{7}$$

where β_0 is the intercept, β_1 is the slope, and ϵ_i is a residual term. Comparison with Eq. (3) indicates that

$$\beta_1 = -2\pi G\rho \tag{8}$$

and therefore

$$\hat{\rho}_P = -\frac{\beta_1}{2\pi G} \tag{9}$$

The negative sign follows the convention adopted in Eq. (3), in which the Bouguer correction is subtracted from the gravity quantity. When an alternative gravity or correction convention is used, the operational sign of the estimator must be adjusted accordingly.

Under ordinary least squares, the regression slope is estimated as

$$\hat{\beta}_1 = \frac{\sum_{i=1}^{N}\left(h_i - \overline{h}\right)\cdot\left(\Delta g_i - \overline{\Delta g}\right)}{\sum_{i=1}^{N}\left(h_i - \overline{h}\right)^2} \tag{10}$$

which leads to the Parasnis density estimator

$$\hat{\rho}_P = -\frac{1}{2\pi G}\cdot\frac{\sum_{i=1}^{N}\left(h_i - \overline{h}\right)\cdot\left(\Delta g_i - \overline{\Delta g}\right)}{\sum_{i=1}^{N}\left(h_i - \overline{h}\right)^2} \tag{11}$$

Equivalently, using covariance and variance notation,

$$\hat{\rho}_P = -\frac{1}{2\pi G}\cdot\frac{\mathrm{Cov}(\Delta g, h)}{\mathrm{Var}(h)} \tag{12}$$

This analytical formulation provides an objective and computationally efficient density estimate. Its simple regression structure makes the Parasnis method particularly suitable for repeated calculations over multiple subsets of observations. The sign convention adopted in Eqs. (9)–(12) follows the formulation introduced in Eq. (3) and must remain consistent throughout the implementation and interpretation.

2.4 Extension to local spatial estimation

Although the Nettleton and Parasnis methods are classically applied to profiles or complete observation sets, the Parasnis formulation can be extended naturally to two-dimensional gridded datasets through local moving-window analysis. In this approach, each grid node is treated as the center of a spatial neighborhood containing paired elevation and gravity values. Density is then estimated from the local covariance between topography and gravity anomaly within that neighborhood. For a moving window centered at node k, the local density estimate is expressed as

$$\hat{\rho}_{P,k} = -\frac{\sum_{i\in W_k}\left(h_i - \overline{h_k}\right)\cdot\left(\Delta g_i - \overline{\Delta g_k}\right)}{2\pi G\sum_{i\in W_k}\left(h_i - \overline{h_k}\right)^2} \tag{13}$$

where W_k denotes the set of observations contained in the window centered at node k, while $\overline{h_k}$ and $\overline{\Delta g_k}$ are the corresponding local mean elevation and local mean gravity anomaly.

Equation (13) is mathematically equivalent to the global Parasnis estimator; only the spatial support of the calculation changes from a complete profile or observation set to a local neighborhood. Repeating the estimation for each valid grid node produces a spatially distributed empirical density field rather than a

single representative value. This local formulation is particularly relevant for heterogeneous shallow environments, in which soil, regolith, and weathered materials may exhibit substantial lateral variability. The moving-window approach therefore provides a practical framework for mapping relative density variations over gridded synthetic and real datasets (De Benedetto et al. 2012; Driba et al. 2024; Garré et al. 2021; Ramos et al. 2026; Romero-Ruiz et al. 2018, 2025).

3 SYNTHETIC TEST FOR VALIDATION

A synthetic test was conducted to evaluate the proposed workflow under controlled conditions in which the reference density field was known a priori. This validation stage allowed direct comparison between the prescribed and estimated density distributions and assessment of whether the local Parasnis formulation could recover the dominant spatial organization of the modeled shallow materials. The analysis was centered on a single two-dimensional experiment because the main objective of the study was to investigate spatially distributed density estimation over gridded domains rather than to develop additional profile-based synthetic cases.

The synthetic model was defined on a regular grid of 81×81 nodes, totaling 6561 points over an area of 40×40 km. The $x-$ and $y-$coordinates ranged from 0 to 40,000 m, with a grid spacing of 500 m. The model was designed to represent a laterally variable shallow environment, with spatial contrasts expressed through topography, density, and the corresponding gravity response. This configuration was adopted because a heterogeneous model is more representative of the spatial variability expected in natural near-surface settings, where density rarely behaves as a laterally uniform parameter.

The synthetic topographic field was constructed to include smooth but spatially distinct relief domains, allowing the gravity–topography relationship to vary across the modeled area. Based on this topography, a reference density field was prescribed to represent shallow-material domains with different physical properties. The resulting density values ranged from 2638.62 to 2818.61 kg m-3, with a mean of 2670.00 kg m-3 and a standard deviation of 43.28 kg m-3. Synthetic gravity was then generated from the combined effects of topography and density, with Gaussian noise of 0.05 mGal added to produce a more realistic controlled scenario. In this model, topography ranged from −79.69 to 299.81 m, whereas synthetic gravity ranged from −11.08 to 68.95 mGal.

In addition to the continuous density field, an initial thematic classification was defined from the prescribed density intervals to group the model into spatial domains with distinct physical behavior. This thematic product was not intended to represent a formal soil or geological classification, but rather a simplified interpretative scheme based on relative density contrasts within the modeled shallow subsurface. Its inclusion in the synthetic experiment allowed the evaluation to consider not only the numerical recovery of density values but also the extent to which the estimated field preserved the principal spatial

compartments of the reference model. Figure 1 presents the reference products of the synthetic experiment, including the synthetic topography, the prescribed density field, the corresponding synthetic gravity response, and the initial thematic classification adopted as an interpretative benchmark.

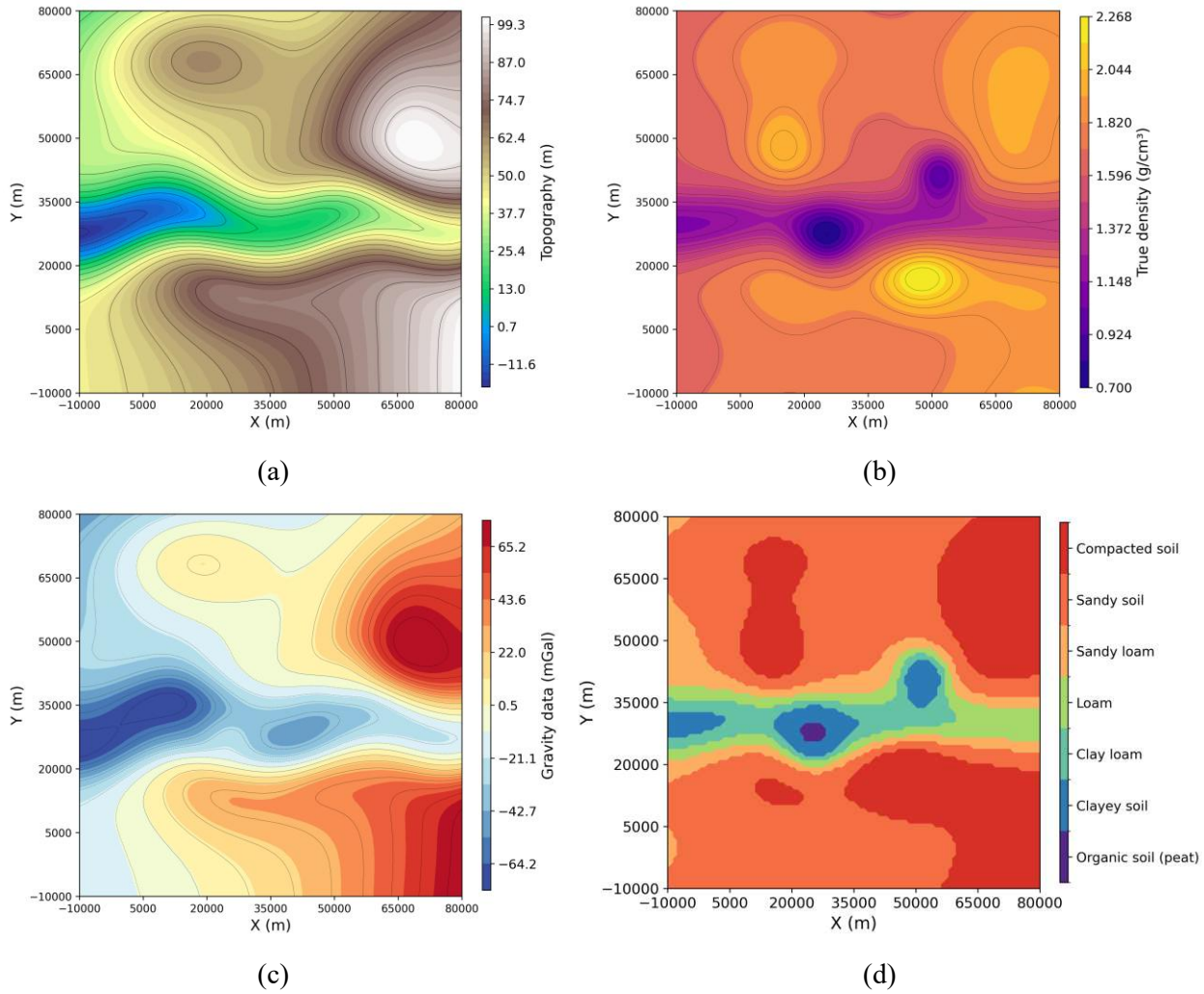
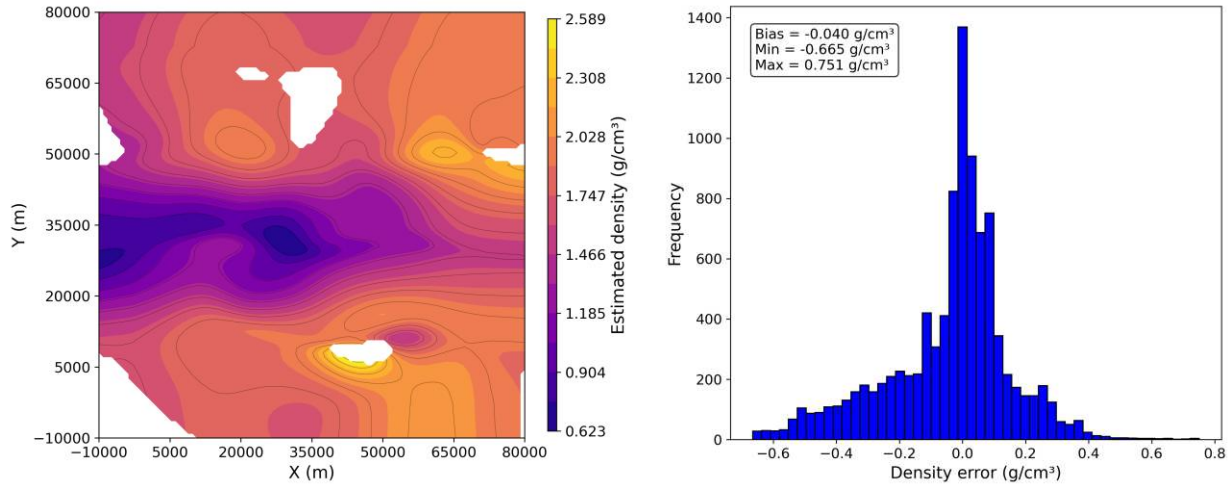


Figure 1: Reference products of the synthetic experiment: (a) synthetic topography, ranging from −79.69 to 299.81 m; (b) prescribed density field, ranging from 2638.62 to 2818.61 kg m^{-3}, with a mean of 2670.00 kg m^{-3} and a standard deviation of 43.28 kg m^{-3}; (c) synthetic gravity field generated from the combined effects of topography and density, including Gaussian noise of 0.05 mGal, and ranging from −11.08 to 68.95 mGal; and (d) initial thematic classification derived from the prescribed density intervals and adopted as an interpretative reference for evaluating the spatial recovery of the proposed workflow

The local Parasnis method was applied to the synthetic grid using square moving windows centered on each node. Because the purpose of the synthetic experiment was to evaluate spatial recovery, the workflow produced pointwise estimates of density and local correlation throughout the grid. A window-

sensitivity analysis was also performed to identify the most stable configuration for the local regression. Moving windows of 5×5, 7×7, 9× 9, 11×11, and 13×13 nodes were evaluated. The corresponding solutions were compared in terms of mean estimated density, standard deviation, mean local correlation, root mean square error (RMSE), mean absolute error (MAE), and number of valid estimates. This comparison allowed the influence of the spatial support of the regression on the stability and accuracy of the estimated density field to be assessed.

The best overall performance was obtained with the 13×13 moving window, which provided the most stable local regression and the most favorable global error metrics among the tested configurations. For this solution, all 6561 grid nodes were successfully estimated. The resulting density field had a mean of 2634.73 kg m^{-3} and a standard deviation of 144.41 kg m^{-3}, while the mean local correlation was 0.9952. The MAE was 102.34 kg m^{-3}, and the RMSE was 153.48 kg m^{-3}. These results indicate that the method does not reproduce the reference field exactly at every node, which is expected in a heterogeneous model where density varies laterally within the moving windows. Figure 2 summarizes the main results obtained with the selected 13×13 moving window. The estimated density field illustrates the spatial organization recovered by the local Parasnis method, whereas the error histogram summarizes the pointwise deviations between the estimated and prescribed density values.



(a) (b)

Figure 2: Main results of the selected synthetic solution obtained with the 13×13 moving window: (a) estimated density field, with a mean of 2634.73 kg m^{-3} and a standard deviation of 144.41 kg m^{-3}; and (b) histogram of pointwise density-estimation errors relative to the prescribed reference field, showing the distribution of local deviations over all grid nodes

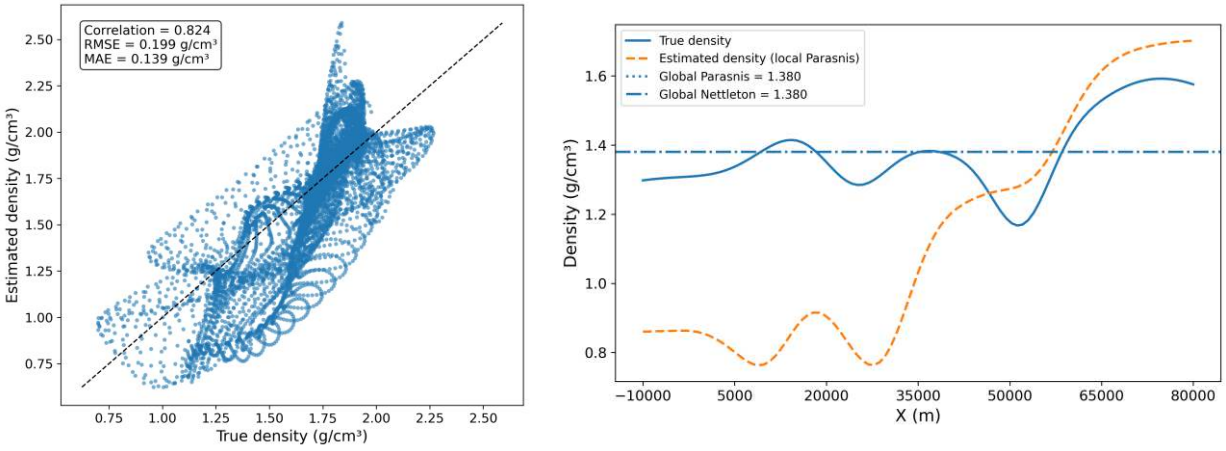
Although the global error metrics improved as the moving-window size increased, the pointwise Pearson correlation between the prescribed and estimated density fields over the complete grid remained low, at 0.0333. This result indicates that the local Parasnis method was more effective in recovering the

dominant spatial compartments of the synthetic model than in reproducing the exact density value assigned to each individual node. This distinction is important because the proposed workflow is intended primarily to identify coherent spatial patterns and relative density contrasts rather than to provide exact pointwise reconstruction in strongly heterogeneous environments.

To complement the grid-scale assessment, a representative profile was extracted from the synthetic model to compare the prescribed density variation with the local Parasnis estimates and the global solutions obtained using the Nettleton and Parasnis methods. The profile-based analysis provides a more direct representation of the differences between a single representative density and a spatially varying estimate derived from local regression. The relationship between the prescribed and locally estimated density values along the selected profile was also examined through a scatter plot, providing complementary measures of agreement for this specific transect.

Along the selected profile, the global Parasnis and Nettleton methods converged to the same representative density of 1.380 g cm^{-3}, confirming the consistency of the two classical formulations under the synthetic configuration considered here. However, because both global methods return a single value for the entire observation set, they cannot represent the lateral density variations prescribed in the reference model. In contrast, the local Parasnis solution captured part of the spatial trend of the reference density, although deviations in amplitude and offset remained along some portions of the profile. This behavior reinforces the distinction between global representative-density estimation and local spatial density recovery, which constitutes the central methodological focus of the study.

Figure 3 presents the local correlation profile together with the density comparison along the extracted section. The local correlation profile identifies portions of the transect where the gravity–topography relationship is more stable, whereas the density-comparison profile shows that the global Parasnis and global Nettleton methods converged to nearly the same representative density, both equal to 1.380 g/cm³.



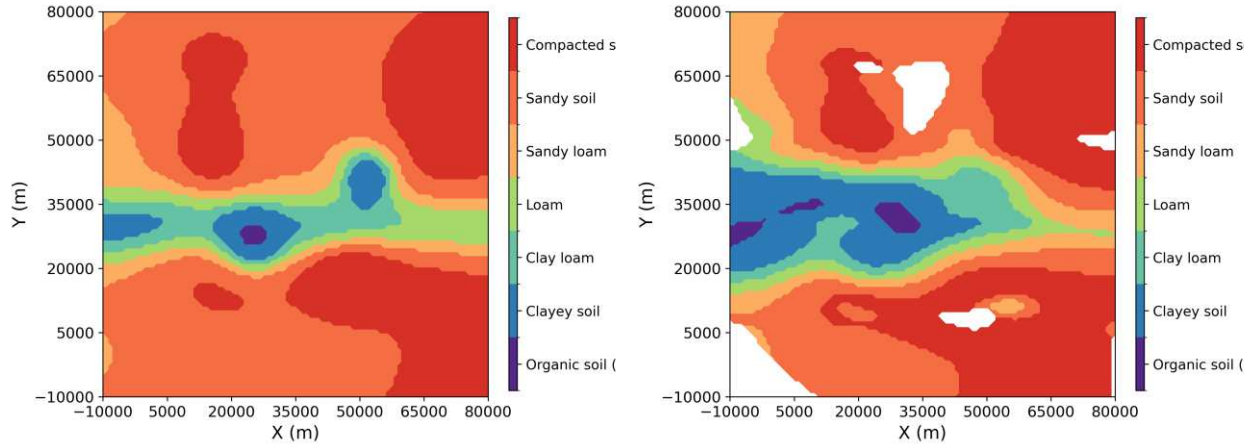
(a) (b)

Figure 3: Profile-based evaluation extracted from the synthetic model: **a** scatter plot comparing the prescribed density and the local Parasnis estimates along the selected profile, with $r = 0.824$, $RMSE = 0.199$ g cm$^{-3,}$ and $MAE = 0.139$ g cm^{-3}; and **b** comparison between the prescribed density variation, the local Parasnis estimate, and the global Parasnis and Nettleton solutions. The two global methods converged to the same representative density of 1.380 g cm^{-3}, whereas the local Parasnis solution captured part of the lateral variability of the reference field.

3.1 Implications for density-based thematic classification

An important outcome of the synthetic analysis was the recovery of the main thematic pattern associated with the reference density model, even though the pointwise density errors were not negligible. In many near-surface applications, the most relevant result is not necessarily the exact reconstruction of density at every grid node, but the identification of spatially coherent zones characterized by relatively lower or higher density values. Such contrasts may reflect differences in material organization, compactness, porosity trends, or other physically relevant properties of the shallow subsurface.

Figure 4 compares the reference thematic classification of the synthetic model with the classification derived from the estimated density field. Despite the local deviations observed in the continuous density estimates, the two maps exhibit similar large-scale spatial compartmentalization. This comparison indicates that the moving-window workflow preserved the dominant organization of the density-based domains represented in the synthetic model.



(a) (b)

Figure 4: Comparison between the density-based thematic classifications of the synthetic model: a reference classification derived from the prescribed density field; and b classification derived from the locally estimated density field. The comparison shows that the moving-window workflow preserved the dominant spatial compartments of the reference model, despite local deviations in the continuous density estimates

This result is particularly relevant to the real-data application because no independent reference density map is available for direct comparison in the Altamira region. Under such conditions, the recovery of spatially coherent density-based domains provides complementary support for interpreting the empirical density field. The synthetic experiment therefore strengthens the methodological basis of the study by showing that local gravity–topography regression can support spatial density mapping and preliminary compartmentalization of shallow materials, even when exact pointwise recovery is limited.

It should be emphasized, however, that the thematic classes used in the synthetic experiment represent simplified density-based compartments rather than formal pedological or geological units. Therefore, the similarity between the reference and estimated classifications should be interpreted as evidence that the workflow preserved the dominant spatial organization of the modeled density contrasts, rather than as a definitive classification of shallow materials. Nevertheless, this result supports the use of the proposed approach as an exploratory tool for identifying spatial domains associated with relative density variations in near-surface investigations.

4 RESULTS AND DISCUSSION

4.1 Study area

The real-data application was conducted in the Altamira region, located in the southwestern portion of the state of Pará, northern Brazil, within the eastern Amazon domain. The study area occupies a broad landscape influenced by the Xingu River basin and by geomorphological conditions characteristic of Amazonian lowlands and adjacent dissected terrains. Its large spatial extent and environmental heterogeneity provide a suitable setting for evaluating spatial variations in density-related properties derived from topographic and gravimetric data. The geographic location and regional extent of the analyzed domain are shown in Fig. 5.

From a geomorphological perspective, the study region includes low-relief to moderately dissected surfaces shaped by fluvial processes, intense tropical weathering, and strong hydrological control on landscape evolution. These factors contribute to substantial lateral variability in the organization and physical properties of shallow materials. In this context, topographic and gravity data provide complementary information on relief and mass-related contrasts, allowing the local gravity–topography relationship to be investigated across the regional domain.

Shallow materials in the Altamira region are associated with intensely weathered tropical environments and commonly exhibit deep alteration profiles and marked lateral variability controlled by relief position, drainage conditions, sedimentary cover, and weathering history. Depending on the local geomorphological and depositional setting, these materials may present contrasting texture, structure, drainage behavior, and physical consistency, all of which may influence the spatial density pattern. The region therefore provides

a relevant setting for testing the proposed empirical density-estimation workflow. Nevertheless, the present study focuses on density-related spatial contrasts, whereas any geological, environmental, or soil-related interpretation is treated as preliminary and indirect.

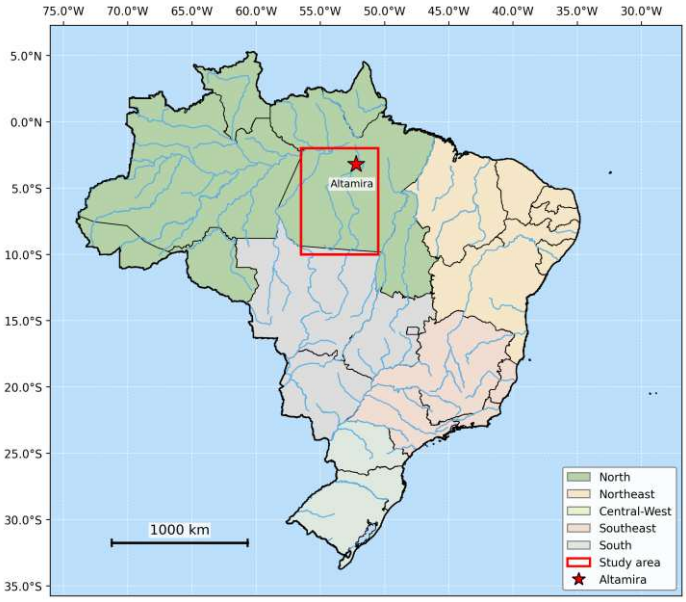


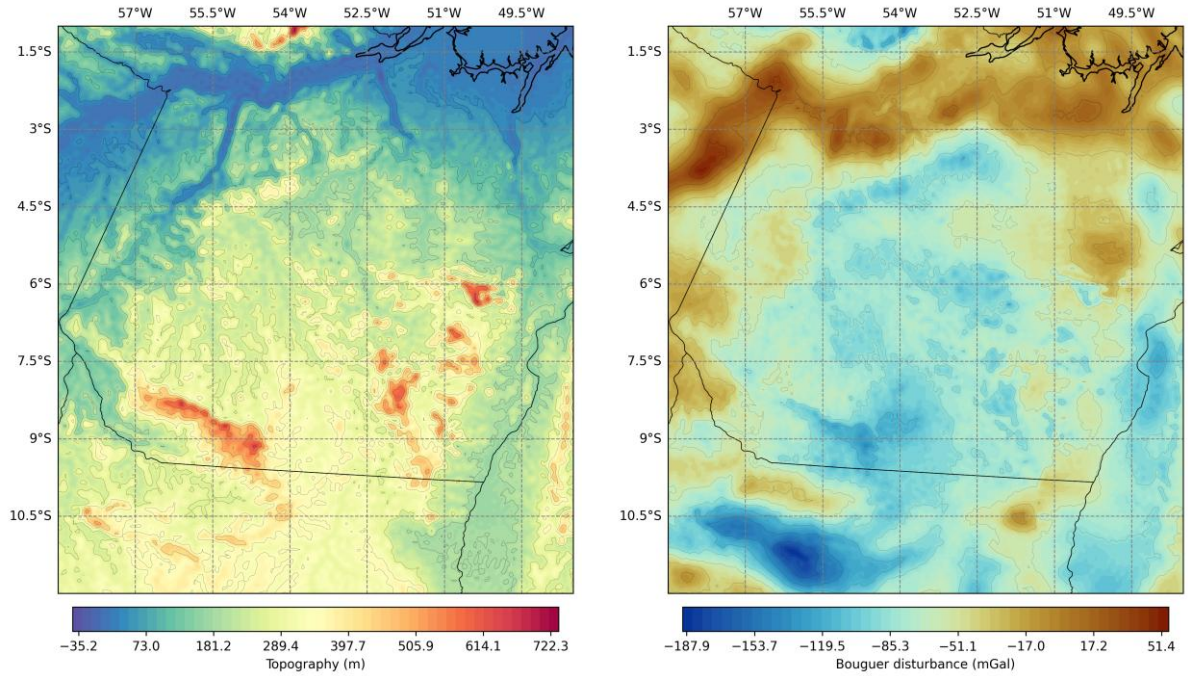
Figure 5 Geographic location of the study area in northern Brazil. The map shows the position of Altamira and the regional extent of the domain analyzed using topographic and gravimetric data

4.2 Real-data workflow

The real-data application was based on gridded topographic and gravimetric datasets covering the Altamira study region. The topographic dataset represented the spatial variability of surface elevation, whereas the gravimetric input consisted of the Bouguer gravity field. These two variables constitute the fundamental inputs of the empirical density-estimation workflow because the local Parasnis approach uses their covariance structure within moving spatial windows.

Before density estimation, the topographic and gravimetric datasets were organized on a common regular grid to ensure pointwise spatial correspondence between elevation and gravity values. This preprocessing step was required because each local regression window must contain paired observations referenced to the same spatial nodes. After grid consistency was verified, the local Parasnis method was applied node by node across the study area using square moving windows, producing an empirical density estimate and an associated local correlation value for each valid grid position.

Figure 6 presents the two input fields used in the real-data application. The topographic map shows the regional distribution of surface elevation, whereas the Bouguer gravity map represents the gravimetric field from which empirical density information was extracted through its local relationship with topography.



(a) (b)

Figure 6: Input datasets used in the real-data application: a topographic field of the study area; and b Bouguer gravity field used as the gravimetric input for local empirical density estimation

As in the synthetic analysis, the local Parasnis formulation was adopted because it allows density to be estimated from the spatially variable relationship between gravity and topography rather than from a single representative value for the entire area. This characteristic is particularly relevant in heterogeneous shallow environments, where lateral variations are expected and a global density estimate may not adequately represent the spatial complexity of the subsurface. The initial density field obtained from the local regressions was therefore evaluated according to physical plausibility criteria.

In real-data applications, local statistical estimates may occasionally produce density values that are incompatible with realistic near-surface materials, particularly in areas where the gravity–topography relationship is weak, noisy, or influenced by geological effects not represented explicitly in the simplified regression model. For this reason, physically based screening and constraint procedures were applied to the estimated field to remove or limit implausible values and retain density ranges considered suitable for interpretation. This procedure converted the direct output of the local regression into a more physically consistent spatial product.

In addition to the empirical density field, the workflow produced a local correlation map that was used as an auxiliary indicator of the stability of the gravity–topography relationship across the study area. Because no independent reference density map was available for direct validation, the joint interpretation

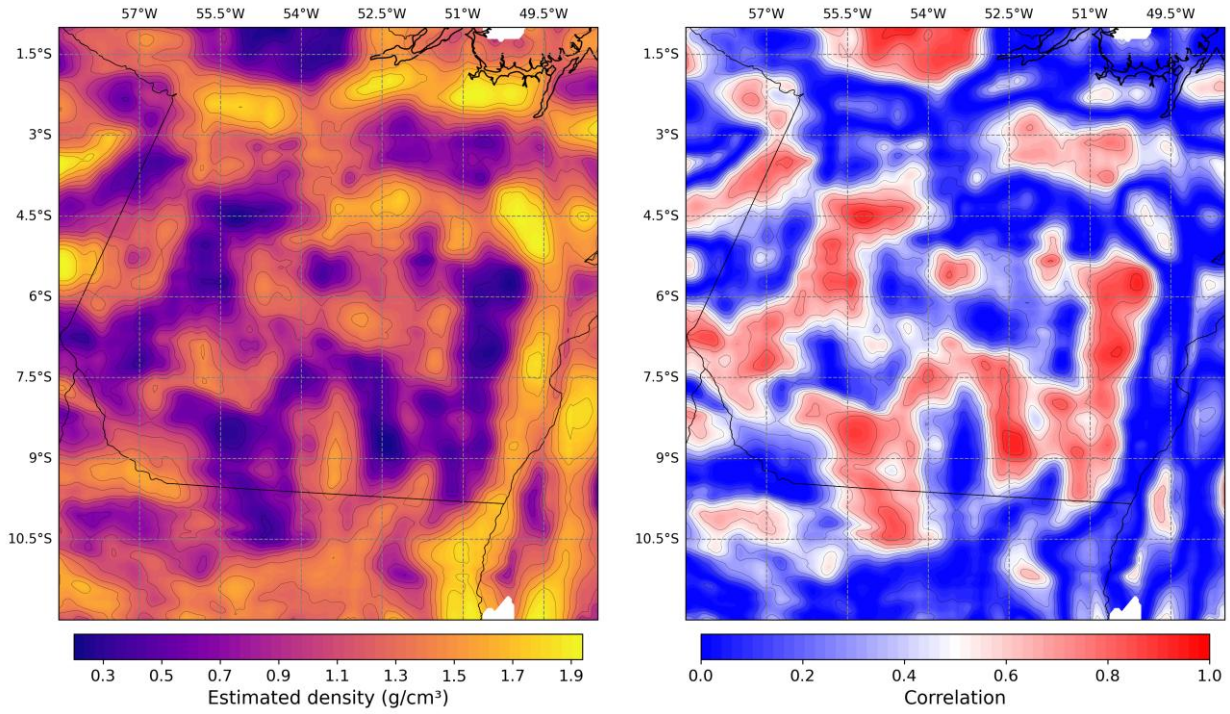
of density and local correlation was essential for assessing the internal consistency of the results. The final outputs of the real-data workflow therefore consisted of the physically constrained empirical density field and the corresponding local correlation map, which form the basis of the spatial analysis presented in the following section.

4.3 Spatial density patterns derived from the Parasnis approach

The application of the local Parasnis method to the real dataset produced a spatially distributed empirical density field and a corresponding local correlation map, which constitute the main interpretative products of the study. Unlike the synthetic experiment, no reference density model was available for direct pointwise comparison. Therefore, the real-data results were evaluated in terms of the spatial coherence of the estimated field, the physical plausibility of the recovered values, and the consistency between the density distribution and the associated local correlation pattern.

The initial density estimates obtained from the local regressions revealed spatial structure but also included values that were incompatible with realistic near-surface materials. Such behavior may occur in real applications because the local gravity–topography relationship can be affected by noise, lateral heterogeneity, regional geological contributions, and reduced statistical stability within some moving windows. Consequently, the raw density output was not interpreted directly. Instead, physical plausibility constraints were applied to suppress unrealistic values while preserving the most consistent components of the spatial pattern.

After applying these constraints, the final empirical density field exhibited a coherent regional organization composed of laterally variable domains that indicate spatial differences in the physical characteristics of the shallow subsurface. Figure 7 presents the constrained density field together with the local correlation map obtained from the same moving-window analysis. The density map highlights the spatial compartmentalization of the study area in terms of relative density contrasts, whereas the correlation map indicates where the local gravity–topography relationship is more stable and the corresponding density estimates are statistically more consistent.

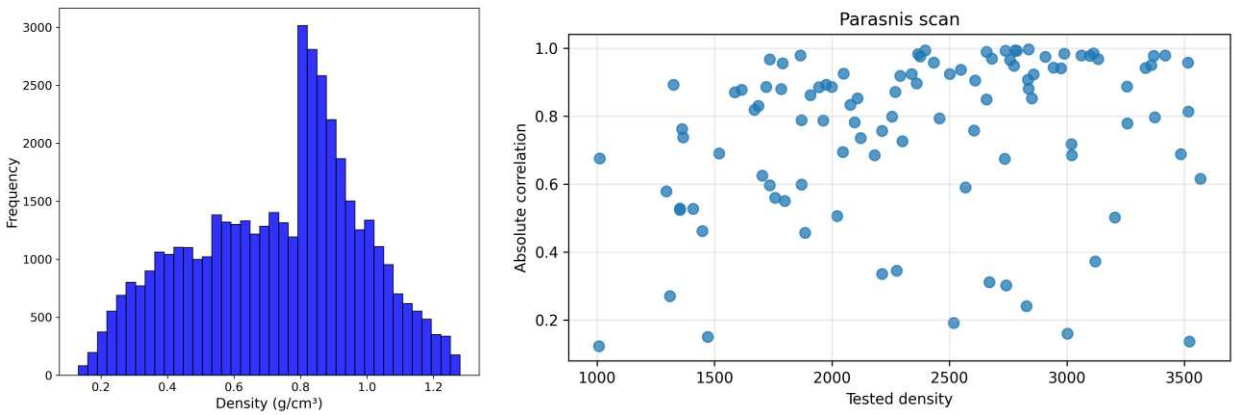


(a) (b)

Figure 7: Main outputs of the real-data application: a spatially distributed empirical density field estimated using the local Parasnis method after the application of physical plausibility constraints; and b local correlation map associated with the gravity–topography relationship within each moving window, used as an auxiliary indicator of the statistical consistency of the density estimates

To complement the map-based interpretation, the real-data results were examined using a statistical summary of the constrained density field and a density scan derived from the gravity–topography relationship. These complementary analyses provide two additional perspectives on the solution: the histogram describes the overall distribution and dominant intervals of the estimated density values, whereas the density scan shows how the absolute correlation varies across the range of tested densities.

Figure 8 presents these complementary products. The histogram summarizes the distribution of the empirical density values retained after the application of physical plausibility constraints, allowing the dominant density intervals and the overall spread of the solution to be evaluated. The density scan displays the variation in absolute gravity–topography correlation as a function of the tested density and identifies the representative value associated with the minimum residual correlation. Together, these products support the statistical interpretation of the spatial density field obtained from the moving-window analysis.



(a) (b)

Figure 8: Complementary statistical products of the real-data application: a histogram of the final empirical density values retained after the application of physical plausibility constraints, showing the dominant density intervals and the overall distribution of the solution; and b density scan showing the absolute gravity–topography correlation obtained for the tested density values, with the representative density identified by the minimum residual correlation.

The local correlation map remains particularly important for interpreting the real-data results because it provides an auxiliary measure of the consistency of the gravity–topography relationship within each moving window. Areas with higher correlation magnitude indicate a stronger local linear association between topography and the Bouguer gravity field, whereas lower-correlation areas suggest that the local regression is more strongly influenced by noise, weak topographic control, or additional geological contributions. The empirical density map should therefore be interpreted jointly with the local correlation field rather than as an isolated spatial product.

From a spatial perspective, the estimated density field exhibits organized domains with relatively distinct density levels rather than an irregular distribution of isolated values. This regional compartmentalization indicates that the local Parasnis analysis is sensitive to spatial variations in the gravity–topography relationship and can delineate relative mass-related contrasts across the study area. The recovered pattern is consistent with the expected heterogeneity of the Altamira region, where relief, drainage, weathering, sedimentary organization, and regional geological structure may contribute to lateral variations in the physical properties of shallow materials. The empirical density field therefore provides a first-order representation of spatial heterogeneity derived from the local relationship between topography and the Bouguer gravity field.

Nevertheless, the results must be interpreted with appropriate caution. The estimated field is empirical and depends on the simplifying assumption that a relevant component of the local gravity variation is related to topographic mass effects within the selected moving window. Regional and deeper geological sources,

data resolution, noise, and variations in the stability of the local regression may also influence the recovered values. Consequently, the estimates should not be regarded as direct measurements of soil or rock density, but as spatially distributed indicators of relative mass-related contrasts. Within these limitations, the combination of physical plausibility constraints, spatial compartmentalization, and correlation-supported interpretation indicates that the local Parasnis approach provides a useful exploratory framework for density mapping in heterogeneous environments.

4.4 Interpretative implications for thematic soil mapping

Although the primary objective of this study is the empirical estimation of near-surface density, the spatial organization of the final density field also provides a basis for preliminary compartmentalization of shallow materials. A laterally coherent density field can be used to delineate domains with contrasting physical behavior and thereby support broader geological, environmental, and pedological interpretations. Density alone, however, is insufficient to define formal soil or geological classes. The mapped compartments should therefore be regarded as first-order spatial domains characterized by relative differences in empirical density.

In the Altamira application, the estimated density field revealed organized spatial domains that may reflect variations in compactness, porosity tendency, degree of weathering, sedimentary arrangement, drainage influence, and other near-surface controls. From this perspective, the map provides a thematic representation of relative physical contrasts across the study area rather than a direct classification of specific materials. Such a product may be particularly useful in regional exploratory investigations, where direct observations are spatially limited and geophysical information can help identify priority areas for subsequent field surveys and more detailed local analyses.

Figure 9 presents the preliminary density-based spatial zoning derived from the empirical density field estimated for the Altamira region. The mapped classes convert the continuous density solution into discrete interpretative compartments, facilitating visualization of the principal regional contrasts. The class names shown in the figure should be understood as qualitative descriptors associated with empirical density intervals and not as direct identifications of soil texture, composition, or compaction state. Accordingly, the map represents an exploratory geophysical product intended to support subsequent interpretation and field verification.

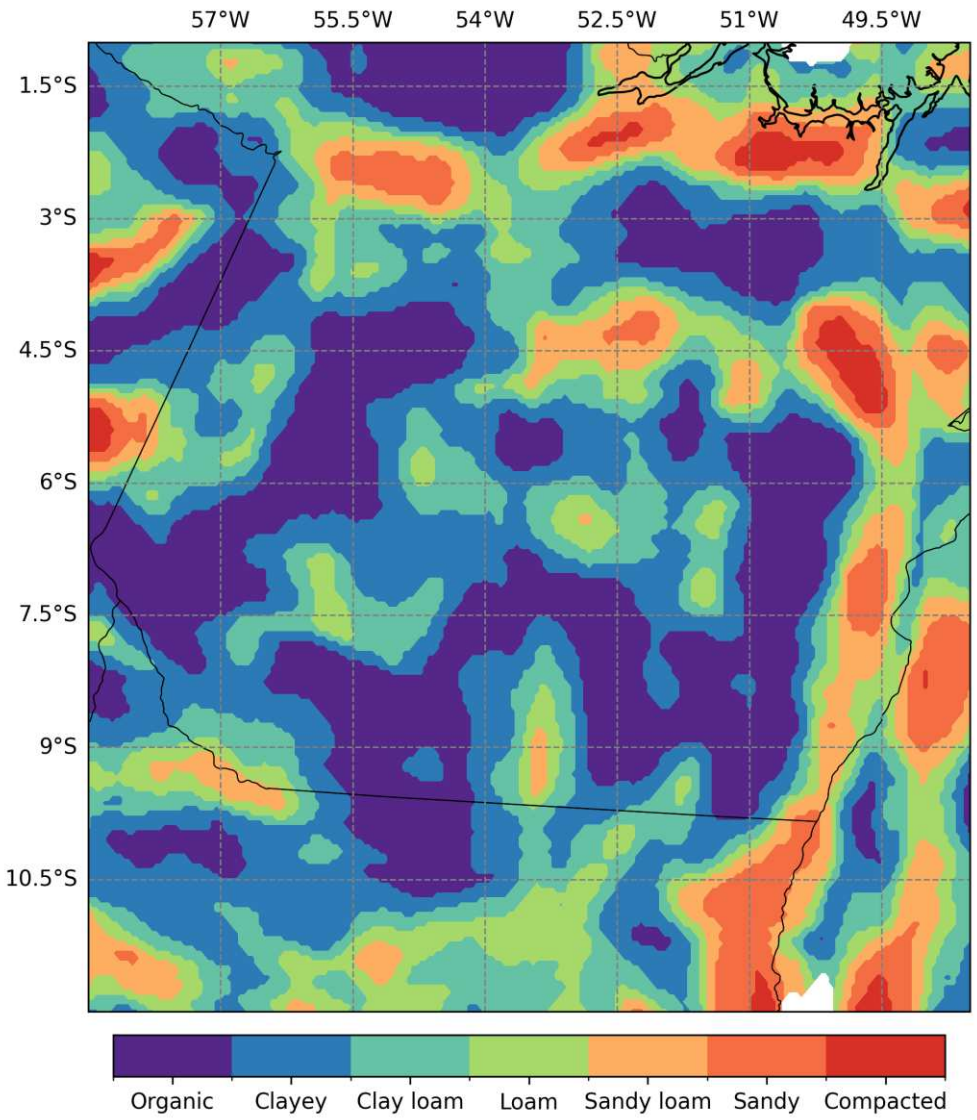


Figure 9: Preliminary density-based spatial zoning derived from the empirical density field estimated for the Altamira region. The mapped compartments represent relative domains of shallow physical contrast. The class names are qualitative interpretative descriptors associated with empirical density intervals and should not be regarded as formal pedological or geological classifications

This interpretative perspective is supported by the synthetic analysis presented earlier in the manuscript. In the controlled experiment, the moving-window workflow recovered the dominant density-based compartments of the reference model, even though the pointwise correspondence between prescribed and estimated values was not exact. This result indicates that the method can preserve large-scale spatial organization despite local estimation errors. In the real-data application, where no independent reference

density field is available, the synthetic results provide methodological support for interpreting the recovered compartments as spatially informative patterns rather than as arbitrary products of the regression procedure.

Density-based interpretation is also relevant because density is physically related to several properties of shallow materials. In qualitative terms, lower-density domains may be associated with greater porosity, reduced compactness, higher weathering intensity, or increased organic content, whereas higher-density domains may indicate more compact, less porous, or mechanically more resistant materials. These relationships are not unique, however, because density is controlled by multiple factors, including lithology, mineral composition, moisture content, pore structure, and depth. Consequently, the mapped classes cannot be used independently to determine soil type, texture, or hydrological behavior and should ideally be evaluated together with geological, pedological, geotechnical, or field observations.

Within this framework, the real-data application suggests that the proposed gravity–topography workflow can support not only empirical density estimation but also preliminary spatial zoning of materials characterized by contrasting mass-related properties. This capability may be particularly relevant in tropical regions such as Altamira, where intense weathering, variable drainage conditions, and heterogeneous geological and geomorphological organization contribute to substantial lateral changes in shallow physical properties. Without implying formal soil or geological classification, the final map provides an exploratory representation of the regional spatial organization and may assist in identifying areas for subsequent field investigation and independent validation.

5 Conclusions

This study investigated the empirical estimation of near-surface density from gravity–topography relationships using the classical Nettleton and Parasnis methods, with particular emphasis on extending the Parasnis formulation from representative profile-based estimates to spatially distributed moving-window analysis. The global formulations remain useful for determining a single representative density over a profile or observation set, but they are inherently limited when the objective is to characterize lateral variability in heterogeneous environments. In contrast, the moving-window Parasnis approach provided a computationally simple framework for estimating an empirical density field over gridded datasets.

The synthetic experiment showed that the proposed workflow preserved the dominant spatial organization of the prescribed density model, although the pointwise correspondence between the reference and estimated values was not exact. This distinction is important because the principal contribution of the method lies in identifying coherent density-related spatial domains rather than reproducing every local density value precisely. The synthetic analysis also demonstrated that the main thematic compartments of the reference model could be recovered despite local estimation errors, supporting the use of the approach for exploratory spatial compartmentalization.

In the Altamira application, the method produced a laterally organized empirical density field consistent with the expected physical heterogeneity of a tropical weathered environment. Because no independent density dataset was available for direct validation, the real-data results were interpreted based on the spatial coherence of the estimated field, the auxiliary information provided by the local correlation map, and the application of physical plausibility constraints to suppress unrealistic values. Under these conditions, the final density field provided a first-order representation of relative mass-related contrasts across the regional study area.

Although the study did not aim to establish a formal soil or geological classification, the spatial organization of the empirical density field also showed potential for supporting preliminary density-based zoning of shallow materials. This result suggests that gravity–topography analysis may provide useful spatial information not only for gravimetric interpretation but also for broader environmental and near-surface investigations, particularly in regions where direct observations are sparse. The resulting compartments should nevertheless be regarded as exploratory geophysical domains requiring independent field verification before any specific material interpretation is assigned.

The limitations of the approach must also be acknowledged. The estimated density field is empirical, depends on the selected moving-window scale, and reflects a simplified representation of the local relationship between gravity and topography. Regional and deeper geological contributions, data resolution, noise, and variations in local regression stability may influence the recovered values. Consequently, the estimates should not be interpreted as direct measurements of soil or rock density, but as spatial indicators of relative mass-related contrasts. Future studies should integrate the proposed workflow with field-density measurements, geological and pedological observations, geotechnical information, or complementary geophysical datasets to evaluate the physical meaning of the mapped domains and improve the robustness of regional interpretations.

Acknowledgments

The first and second authors gratefully acknowledge BASA – Banco da Amazônia S.A. for the financial support provided through the approval of the project under the GERES/CDSU Research Call, formalized by Contract No. 2024/224.

Declaration of Interest

The author declares that there are no financial or non-financial conflicts of interest directly or indirectly related to the research, authorship, or publication of this manuscript.

Funding Information

The authors declare that this research received financial support from BASA – Banco da Amazônia S.A., through the GERES/CDSU Research Call, formalized by Contract No. 2024/224. The funding institution had no role in the study design, data analysis, interpretation of results, manuscript preparation, or decision to submit the work for publication.

Authors Contributions

First author was responsible for the conceptualization, methodological design, computational implementation, data processing, analysis and interpretation of the results, preparation of figures, and writing of the manuscript. The second, third and fourth authors assisted in the development of the study, contributing to the discussion, organization, and interpretation of the results together. First author also supported data organization, computational tests, bibliographic review, and analytical procedures. The third author contributed to the preparation of selected maps and to the provision of supporting materials used in the research. The fourth author contributed to the formulation of the initial research project. All authors read and approved the final version of the manuscript.

Data and Material Availability

The topographic and gravimetric data used in this study were obtained from publicly available global and institutional databases. The gravity field information was obtained from the International Centre for Global Earth Models (ICGEM), using the XGM2019e global gravity field model. The geographic and regional information used to describe the study area was obtained from public institutional reports and spatial datasets. The author gratefully acknowledges the research group GEMATECX – Grupo de Estudos em Matemática e Tecnologia no Xingu,registered in the CNPq Directory of Research Groups (dgp.cnpq.br/dgp/espelhogrupo/3759353252129693), for its institutional, scientific, and collaborative support during the development of this work, particularly in discussions related to mathematics, technology, geosciences, and regional applications in the Xingu region. The processed data, scripts, and figures generated during the development of this study may be made available by the corresponding author upon reasonable request.

References

Barry J. Allred, M. Reza Ehsani, and Jeffrey J. Daniels. General considerations for geophysical methods applied to agriculture. *Handbook of Agricultural Geophysics*, pages 3–16, 2008.

Barry J. Allred, Robert S. Freeland, Hamid J. Farahani, and Mary E. Collins. Agricultural geophysics: Past, present, and future. In *23rd EEGS Symposium on the Application of Geophysics to Engineering*

642 *and Environmental Problems*, pages cp–175. European Association of Geoscientists & Engineers,
643 2010.
644 Barry J. Allred, Viacheslav I. Adamchuk, R. A. Viscarra Rossel, Jim Doolittle, Robert S. Freeland,
645 Katherine R. Grote, Dennis L. Corwin, R. Lal, and R. Lal. Geophysical methods. *Encyclopedia of*
646 *Soil Science*, 3:1–8, 2016.
647 Guilliam Barboza-Miranda, Andrea Carolina Lopez Macías, Jisseth Valdez-Vargas, Meiker Pérez-Barón,
648 Yamid E. Nuñez de la Rosa, Gustavo Eliecer Florez de Diego, Juan José Carrascal, and Jair Arrieta
649 Baldovino. Geophysical-geotechnical characterization of mud volcanoes in Cartagena Colombia.
650 *Geosciences*, 15(3):111, 2025.
651 Richard J. Blakely. *Potential Theory in Gravity and Magnetic Applications*. Cambridge University Press,
652 1996.
653 Guillaume Blanchy, Chris W. Watts, Jake Richards, Jennifer Bussell, Katharina Huntenburg, Debbie L.
654 Sparkes, Mark Stalham, Malcolm J. Hawkesford, W. Richard Whalley, and Andrew Binley. Time-
655 lapse geophysical assessment of agricultural practices on soil moisture dynamics. *Vadose Zone*
656 *Journal*, 19(1):e20080, 2020.
657 Meghan Brown, Robert Heinse, Jodi Johnson-Maynard, and David Huggins. Time-lapse mapping of crop
658 and tillage interactions with soil water using electromagnetic induction. *Vadose Zone Journal*,
659 20(4):e20097, 2021.
660 Alberto Carrera, Ilaria Barone, Mirko Pavoni, Jacopo Boaga, Nicola Dal Ferro, Giorgio Cassiani, and
661 Francesco Morari. Assessment of different agricultural soil compaction levels using shallow seismic
662 geophysical methods. *Geoderma*, 447:116914, 2024.
663 Mihai O. Cimpoiașu, Oliver Kuras, Paul B. Wilkinson, Tony Pridmore, and Sacha J. Mooney.
664 Hydrodynamic characterization of soil compaction using integrated electrical resistivity and X-ray
665 computed tomography. *Vadose Zone Journal*, 20(4):e20109, 2021.
666 D. L. Corwin. Past, present and future trends of soil electrical conductivity measurement using
667 geophysical methods. *Handbook of Agricultural Geophysics*. CRC Press, Boca Raton, FL, pages 17–
668 44, 2008.
669 Jaqueline Vígolo Coutinho. *Caracterização geofísica e modelagem do escoamento subterrâneo em área*
670 *de afloramento do Sistema Aquífero Guarani*. PhD thesis, Universidade de São Paulo, 2019.
671 Felipe Vieira da Cunha, Marcos Gervasio Pereira, Paulo Sérgio dos Santos Leles, and Elton Luiz da Silva
672 Abel. Atributos químicos e físicos do solo em áreas sob diferentes coberturas florestais e pastagem
673 em Além Paraíba-MG. *Ciência Florestal*, 28(1):13–24, 2018.

Daniela De Benedetto, Annamaria Castrignano, Donato Sollitto, Francesca Modugno, Gabriele Buttafuoco, and Giuseppe lo Papa. Integrating geophysical and geostatistical techniques to map the spatial variation of clay. *Geoderma*, 171:53–63, 2012.

Dejene L. Driba, Efemena D. Emmanuel, and Kennedy O. Doro. Predicting wetland soil properties using machine learning, geophysics, and soil measurement data. *Journal of Soils and Sediments*, 24(6):2398–2415, 2024.

Jamshid Farifteh, A. Farshad, and Richard J. George. Assessing salt-affected soils using remote sensing, solute modelling, and geophysics. *Geoderma*, 130(3–4):191–206, 2006.

Ludmila de Freitas, Ivanildo Amorim de Oliveira, José Carlos Casagrande, Laércio Santos Silva, and Milton César Costa Campos. Estoque de carbono de latossolos em sistemas de manejo natural e alterado. *Ciência Florestal*, 28(1):228–239, 2018.

Sarah Garré, Frédéric Nguyen, Nolwenn Lesparre, and Thomas Hermans. The mathematical challenges in agrogeophysics: examples and ways ahead. In *12th Conference on Sustainable Development of Energy, Water and Environment Systems (SDEWES 2017)*, 2017.

Sarah Garré, David Hyndman, Benjamin Mary, and Ulrike Werban. Geophysics conquering new territories: The rise of "agrogeophysics". *Vadose Zone Journal*, 20(4):e20115, 2021.

Mayra Abreu Gouveia and Rosane Cunha Maia Nobre. Mapeamento do índice de risco de contaminação de águas subterrâneas por BTEX em Maceió-AL. *XIII Simpósio de Recursos Hídricos do Nordeste*, 2016.

Paul Groves, Giovanni Cascante, Dave Dundas, and P. K. Chatterji. Use of geophysical methods for soil profile evaluation. *Canadian Geotechnical Journal*, 48(9):1364–1377, 2011.

William J. Hinze, Ralph R. B. Von Frese, and Afif H. Saad. *Gravity and Magnetic Exploration: Principles, Practices, and Applications*. Cambridge University Press, 2013.

Mohsen Hosseinalizadeh, Narges Kariminejad, Abdolreza Bahremand, Najmeh Gangi, Anita Bernatek Jakiel, Hossein Tazikeh, Vahid Shafaie, and Majid Movahedi Rad. Integrating geophysical techniques and UAV mapping for the detection and temporal analysis of soil pipes and pipe collapses in agricultural loess landscapes. *Geoenvironmental Disasters*, 12(1):37, 2025.

Verza Julyani, Lindung Zalbuin Mase, Hardiansyah Hardiansyah, Rena Misliniyati, Khairul Amri, and Suched Likitlersuang. A case study on geophysical characterisation of bedrock depth and soil stratigraphy. *Transportation Infrastructure Geotechnology*, 12(6):173, 2025.

George Kritikakis, Eleni Kokinou, Nikolaos Economou, Nikolaos Andronikidis, John Brintakis, Ioannis N. Daliakopoulos, Nektarios Kourgialas, Aikaterini Pavlaki, George Fasarakis, Nikolaos Markakis, et al. Estimating soil clay content using an agrogeophysical and agrogeological approach: A case study in Chania Plain, Greece. *Water*, 14(17):2625, 2022.

Janine Krüger, Uwe Franko, Johann Fank, Ernest Stelzl, Peter Dietrich, Marco Pohle, and Ulrike Werban. Linking geophysics and soil function modeling—an application study for biomass production. *Vadose Zone Journal*, 12(4):vzj2013–01, 2013.

Alexandria S. Kuhl, Anthony D. Kendall, Remke L. van Dam, Stephen K. Hamilton, and David W. Hyndman. Root water uptake of biofuel crops revealed by coupled electrical resistivity and soil water content measurements. *Vadose Zone Journal*, 20(4):e20124, 2021.

Ronaldo Luna and Houda Jadi. Determination of dynamic soil properties using geophysical methods. In *Proceedings of the First International Conference on the Application of Geophysical and NDT Methodologies to Transportation Facilities and Infrastructure*, St. Louis, MO, pages 1–15, 2000.

A. I. Menshov, A. V. Kruglov, and A. V. Sukhorada. Informational content of the soil magnetism indicators for solving agrogeophysics and soil science tasks. *Scientific Bulletin of National Mining University*, (3), 2012.

Muhammet Nergizci, Ramazan Alpay Abbak, and Muzaffer Ozgu Arisoy. The effect of crustal density heterogeneity on determining gravimetric geoid: Example in central Anatolia, Türkiye. *Journal of Asian Earth Sciences*, 264:106037, 2024.

Lewis L. Nettleton. Determination of density for reduction of gravimeter observations. *Geophysics*, 4(3):176–183, 1939.

Feng-gui Niu, Shi Chen, Yong-bo Li, Hong-lei Li, Yuan-yuan Niu, and Yu-hang Pan. Simultaneous estimation of Bouguer gravity anomaly and near-surface density using Bayesian approach: A Yunnan case study. *Applied Geophysics*, 22(4):1109–1124, 2025.

Dave O'Leary, Patrick Tuohy, Owen Fenton, Mark G. Healy, Hilary Pierce, Asaf Shnel, and Eve Daly. Assessing the impact of rewetting agricultural fen peat soil via open drain damming: an agrogeophysical approach. *Soil*, 12(1):151–164, 2026.

Nuris Orihuela. Método de Parasnis modificado. Aplicación al macizo montañoso del Ávila. *GEOS Revista Venezolana de Ciencias de la Tierra*, (32), 1997.

Eduane José de Pádua, Adriano Ribeiro Guerra, and Yuri Lopes Zinn. Modelagem da densidade do solo em profundidade sob vegetação nativa em Minas Gerais. *Revista Brasileira de Ciência do Solo*, 39(3):725–736, 2015.

D. S. Parasnis. *Principles of Applied Geophysics*. Chapman & Hall, London, 5 edition, 1997.

Lianne Borja Pimenta. *Espacialização das áreas favoráveis à expansão da fronteira agrícola no Estado do Pará: uma avaliação multicritério apoiada por geoprocessamento*. PhD thesis, Programa de Pós-Graduação em Ciências Ambientais, 2018.

Julián Ramos, Nestor Bonomo, Claudio García, and Andrés Quincke. Agrogeophysical approach to estimate soil A horizon thickness in a long-term dryland cropping experiment in South America. *Soil Systems*, 10(3):36, 2026.

Alejandro Romero-Ruiz, Niklas Linde, Thomas Keller, and Dani Or. A review of geophysical methods for soil structure characterization. *Reviews of Geophysics*, 56(4):672–697, 2018.

Alejandro Romero-Ruiz, Dave O'Leary, Dongxue Zhao, Yuxin Wu, and Sarah Garré. Preface: Illuminating soil's hidden dimensions, a decade of progress and future directions in agrogeophysics research. *Soil*, 11(2):1041–1051, 2025.

Kalyan Kumar Roy. *Potential Theory in Applied Geophysics*. Springer Science & Business Media, 2007.

Md Abdus Samad, Leti T. Wodajo, Parsa Bakhtiari Rad, Md Lal Mamud, and Craig J. Hickey. Integrated agrogeophysical approach for investigating soil pipes in agricultural fields. *Journal of Environmental and Engineering Geophysics*, 27(4):207–217, 2022.

Simon Sadok Siregar, Tetti Novalina Manik, Nur Maulida, Tarisa Ananda, Ninis Hadi Haryanti, Sudarningsih Sudarningsih, et al. Mineralogical and geophysical properties of peat soil for sustainable urban development in South Kalimantan, Indonesia. *Engineering, Technology & Applied Science Research*, 16(1):30759–30767, 2026.

William Murray Telford, L. P. Geldart, and Robert E. Sheriff. *Applied Geophysics*, volume 1. Cambridge University Press, 1990.

Cleilson Nascimento Uchôa, Edson Ampélio Pozza, Adélia Aziz Alexandre Pozza, and Wilson da Silva Moraes. Modelagem geoestatística da sigatoka-negra e sua relação com a fertilidade do solo. *Bioscience Journal*, 27(3):357–362, 2011.

Christian von Hebel, Sophie Reynaert, Klaas Pauly, Pieter Janssens, Isabelle Piccard, Jan Vanderborght, Jan van der Kruk, Harry Vereecken, and Sarah Garré. Toward high-resolution agronomic soil information and management zones delineated by ground-based electromagnetic induction and aerial drone data. *Vadose Zone Journal*, 20(4):e20099, 2021.